

UNCLASSIFIED

AD NUMBER
AD864750
NEW LIMITATION CHANGE
TO Approved for public release, distribution unlimited
FROM Distribution authorized to U.S. Gov't. agencies and their contractors; Administrative and Operationa Use, Export Control; Jan 1970. Other requests shall be referred to Naval Air Systems Command, Patuxent River, MD 20670.
AUTHORITY
NASC, per DTIC Form 55

THIS PAGE IS UNCLASSIFIED

AD 864750

NWC TP 4805  
COPY 90

# STATIC AND DYNAMIC PROPERTIES OF TWO EXPLOSIVE MATERIALS

by

Werner Goldsmith,  
University of California  
Berkeley, California

and

Thomas A. Reitter  
Carl F. Austin  
Research Department

D D C  
RECEIVED  
FEB 10 1970  
RECEIVED  
C

**ABSTRACT.** Test rods of Composition B-3 and TNT were cast 43.2 centimeters long and 2.13 centimeters in diameter. The rods were struck axially by spherical steel projectiles, and symmetric stress wave passage was observed by strain gage arrays. Strain pulses were found to attenuate and disperse with travel distance. Both damaged and undamaged rods were examined microscopically using thin-section techniques and were also tested for static compressive and tensile strength. The thin-section technique was able to show grain and crystal damage resulting from impacts. A macroscopic constitutive equation for these materials must take into account their anelastic behavior.

Reprinted by the  
CLEARINGHOUSE  
for Federal Scientific & Technical  
Information Springfield, Va. 22151



**NAVAL WEAPONS CENTER**  
CHINA LAKE, CALIFORNIA • JANUARY 1970

**DISTRIBUTION STATEMENT**

THIS DOCUMENT IS SUBJECT TO SPECIAL EXPORT CONTROLS AND EACH TRANSMITTAL TO FOREIGN GOVERNMENTS OR FOREIGN NATIONALS MAY BE MADE ONLY WITH PRIOR APPROVAL OF THE NAVAL WEAPONS CENTER.

SUBJECT		
REPORT	WHITE SECTION	<input type="checkbox"/>
DDC	GRAY SECTION	<input checked="" type="checkbox"/>
UNCLASSIFIED		
JUSTIFICATION		
M. R. Etheridge, Capt., USN		
Commander		
By Thomas S. Amlie, Ph.D.		
Technical Director		
DISTRIBUTION/AVAILABILITY STATE		
DIS.	AVAIL.	SPECIAL
2		

# NAVAL WEAPONS CENTER

## AN ACTIVITY OF THE NAVAL MATERIAL COMMAND

### FOREWORD

The material in this report represents part of a continuing applied research program in support of explosive ordnance problems at the Naval Weapons Center. These studies were supported by funds under the Naval Air Systems Command Task Assignment A35-350/216/70 F17353501.

Technical reviewers of this report were D. P. Ankeny of the Systems Development Department, and R. G. S. Sewall of the Weapons Development Department.

Released by  
**JOHN PEARSON, Head**  
 Detonation Physics Division  
 10 December 1969

Under authority of  
**HUGH W. HUNTER, Head**  
 Research Department

NWC Technical Publication 4805

Published by..... Research Department  
 Collation.....Cover, 17 leaves, DD Form 1473, abstract cards  
 First printing.....215 unnumbered copies  
 Security classification.....UNCLASSIFIED

## INTRODUCTION

The static and dynamic properties of explosives become of interest to the warhead design engineer in two principal situations. The first of these arises when the explosive is considered to be part of the physical structure of the warhead; that is, the explosive contributes to the strength of the device, thereby reducing the percentage of inert material in the warhead (Ref. 1 and 2). The second occurs when the warhead must survive an initial impact prior to functioning. With thin-skinned targets the deceleration-imposed shock upon target impact is small, but with bar armor, skirting, or hard targets such as concrete fortifications, the deceleration-imposed shock to the explosive becomes very large to the point of causing premature detonation of the warhead in many cases (Ref. 3, 4, and 5).

In recent years a number of investigations have been conducted to determine both the dynamic and static mechanical properties of a variety of nonmetallic substances. These tests included concrete and epoxy mixtures, plastics, and natural rocks (Ref. 6 through 10). The dynamic information was derived from the passage of stress wave pulses produced by the central longitudinal impact of projectiles, usually hard steel spheres 1.27-centimeters in diameter, at various velocities on ballistically suspended Hopkinson bars composed of the materials being tested. The transient pulses were detected by strain gages mounted in pairs at each of several stations located on the surface of the test rods. The strain gage arrays provided basic data from which wave propagation velocities, pulse decay, and pulse dispersion could be obtained. These values, in turn, permitted the calculation of a dynamic Young's modulus and the limiting tensile strength (determined from the amplitude of waves reflected from the distal end that propagated past known tensile fracture regions). The values also allowed the construction of a one-dimensional constitutive equation based on a very simple model of mechanical behavior.

In these various test series, static tests were conducted on both virgin and mechanically shocked specimens, using standard tensile and compressive equipment. Microscopic examinations of thin sections of the virgin and shocked samples were performed in order to ascertain visually the extent of internal grain and grain-bond damage.

The present series of tests were designed to provide the same stress wave and physical parameter data for two widely used explosives, Composition B and standard TNT (trinitrotoluene). These two explosives represent two extremes: a two-component system composed of fine-grained

crystals in a coarse-grained matrix, and a coarse-grained single-component system. Composition B is a name for a rather widely varying family of explosives. The tests reported were run solely upon Composition B-3, a specific form of Composition B which was chosen because of related and on-going studies in the shock initiation of this explosive (Ref. 11 and 12).

The experimental techniques used were substantially the same as those used in previous studies and described in the open literature (Ref. 13). The explosive nature of the test specimens, however, required some degree of added caution. The upper limit of impact velocity of 150 microseconds, planned for the Hopkinson bar tests, was considered to be well below the anticipated initiation velocity of 610 microseconds for Composition B-3 and 975 microseconds for TNT (Ref. 14). Although no explosions of the test rods occurred during the investigation, all of the dynamic tests using explosive rods were conducted in an explosives test area firing barricade.

#### SPECIMEN MANUFACTURE, PREPARATION, AND REPAIR

Composition B-3 and TNT were the two test materials used. Table 1 presents specifications for the various common designations of Composition B. The test samples used Type II RDX containing 5 to 10% HMX (cyclotetramethylene tetranitramine), which replaced a portion of the normal complement of RDX (cyclotrimethylene trinitramine). Furthermore, 0.5% of alpha-nitronaphthalene was added to the Composition B-3 and 1.0% added to the cast TNT as a cracking inhibitor.

Test specimens of both explosives were cast as rods 43.2 centimeters long and 2.13 centimeters in diameter. The molds used were thin-walled aluminum conduit. The explosive rods shrank sufficiently upon cooling to allow them to be slipped out of the molds.

The first attempt to cast relatively void-free rods of Composition B-3 ended in virtual failure when the resulting rods were found to exhibit coarse flow textures and an extensive retention of bubbles. The rod marked A in Fig. 1 shows this type of rod; the rod marked B shows the satisfactory results of a second pour using a greater degree of preheating of the molds. Casting of satisfactory B-3 rods was done by steam-melting the explosive at a temperature of 102°C and a pressure of 13.0 millimeters of mercury, and then pouring it into aluminum tubes coated with silicone grease, preheated to 91.6°C. Pouring into the molds was done at the ambient atmospheric pressure of approximately 707 millimeters of mercury.

TNT test rods were formed by pouring TNT, melted at a temperature of 85°C and at a pressure of 918 millimeters of mercury, into silicone-grease-coated aluminum tubes preheated to 78.3°C, with the pouring also at ambient atmospheric pressure. Interestingly, the TNT rods exhibited

TABLE 1. Military Specifications for Composition B  
Data provided by Code 45 NWC.

Property or component	Composition B	Composition B-2	Composition B-3a	Composition B-4
RDX, %	60.0 ± 2.0	60	59.5 ± 1.0 (Type II RDX only)	60.0 ± 2.0
TNT, %	39.0 ± 2.3	40	40.5 ± 1.0	39.5 ± 2.0
Desensitizer, %	1.0 ± 0.3	(no wax)	(no wax or desensitizer)	0.5 ± 0.15 calcium silicate
Max. moisture, %	0.25	...	0.25	0.25
Max. acidity, %	RDX I, 0.03 <sup>b</sup> RDX II, 0.02 <sup>c</sup>	RDX I, 0.03 RDX II, 0.02	RDX II, 0.02	RDX I, 0.03 RDX II, 0.02
Viscosity, efflux time, sec.	RDX I, 5.0 ± 2.0 RDX II, 12.0 ± 5.0	...	20.0	9.0
Max. number of insoluble particles retained on No. 60 sieve per 50 g.	5	...	5	5

<sup>a</sup> The primary distinguishing characteristic of Composition B-3 is the smaller RDX particle size which results in greater viscosity; particle size is not specified for other types of Composition B. For B-3 the median particle diameter is 65 to 80 microns.

<sup>b</sup> Type I RDX: nitric acid process; less than 1% HMX.

<sup>c</sup> Type II RDX: acetic anhydride process; up to 12% HMX.

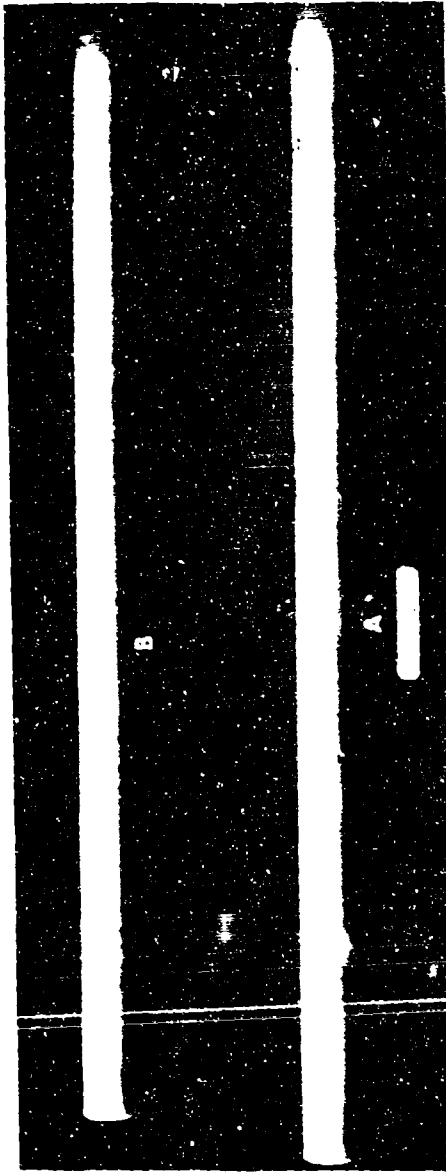


FIG. 1. Two Qualities of Composition B-3 Rod. (A) Unsatisfactory due to retained voids and (B) relatively free of voids and used in tests.



FIG. 2. Typical Grain-Size Variation Exhibited by the Vertically Cast TNT Rods. (A) Fine-grained lower end and (B) coarse-grained upper end.

a steady increase in grain size from the lower end of the rod to the upper end. Figure 2 shows a typical TNT rod with a fine-grained end (A) and coarse-grained (B). The apparent reason for the grain size variation was the slower cooling of the upper portion, primarily due to the presence of the large riser above the cluster of mold tubes.

The specimens to be tested dynamically were carefully scribed in order to mark the position of the strain gage locations at longitudinal intervals of 8.89 centimeters, with the gage locations starting and ending 3.81 centimeters from each end of the test rod. At each longitudinal station two gages were emplaced on the opposite ends of a diameter, with all of the gages on one side along a common straight line, that is, along a single generator of the cylinder. The strain gages were first attached to transparent plastic tape and positioned on the test rod. One side of the tape was lifted, Eastman 910 cement inserted under the gage, and then the gage was pressed onto the explosive rod and held in place by means of the ring of transparent tape until the cement had dried. In spite of the residual silicone-grease film, successful cementing of the gages was accomplished after 24 hours of setting time. The tape was left on the rods as a protection to the strain gages.

Short cylinders of explosive were also made for use as frontal protectors and for use as distal-end wave traps. These terminal pieces were made by taking unshocked sections of larger rods and machining them to the proper length. These shorter cylindrical sections were then glued to both ends of the larger rods with Eastman 910 cement--which was used for all gluing tasks in these tests. For most of the test rods, an additional piece was glued onto the impact end. This piece consisted of a cylinder of 2024-T3 aluminum 1.27 centimeters long, with the same diameter as the test rod. On a few of the test rods, this aluminum cap was omitted in order to determine by comparison the effect of its use both as a protective cap to prevent gross physical shatter of the impact end of the rod and as a possible means of transmitting stress into the test rods more efficiently.

Rods of explosive which were grossly damaged or broken by impact were reassembled and glued back together. The effect of such repair had been previously shown to be negligible for this range of wave lengths. For most tests, the explosive terminal pieces were replaced after each shot; the aluminum cap was always replaced. Although the rods were closely examined visually following each test shot, some of the fractures did not always show. As a result, some specimens with hidden fractures failed during subsequent handling both in the laboratory and while being emplaced for an additional impact. In general, the grain damage caused by impact was more visible macroscopically in the TNT than in the Composition B-3 samples. After an impact, all fracture locations were carefully noted.

Selected test rods were measured and weighed for density determinations. In addition to the instrumented test rods, a number of rods were

left uninstrumented in order to provide additional samples which could be shocked under the identical impact conditions as the instrumented ones. These samples were for future donor receptor initiation studies and for microscopic examination.

With the TNT samples, impact normally was made at the fine-grained end of the rod, though some rods were shocked from the opposite end and from both ends.

Specimens for static tensile and compression tests were prepared from both virgin and shocked rods of Composition B-3 and TNT. The tensile samples were formed by cutting and then flat-facing the ends of pieces of the test rods, to yield a specimen length of 8.26 centimeters. This length was selected as a compromise between the desired sample length of 5 diameters (10.65 centimeters) and the actual sample lengths which could be obtained in usable form from the shocked test rods. A steel cylinder 2.54 centimeters long, with the same diameter as the test specimen (2.13 centimeters), was glued to each end of the tensile sample. The steel cylinders used as tensile test end caps were concentrically drilled and tapped for connection to the tensile test apparatus. Specimens intended for compression tests were machined to a finished length of 5.08 centimeters with the ends parallel to not less than 0.003 millimeter across a diameter and flat to  $\pm 0.007$  millimeter. For all tensile- and compression-test samples that were cut from shocked rods, the orientation and position of the samples with respect to the shocked end were carefully noted.

#### THIN-SECTION PROCEDURE

Detailed microscopy of the shocked explosives was desired as a means of defining the structure of the test rods and illuminating possible damage mechanisms inherent in them. The literature presents microtome and "film and cast" techniques, but these both cause excessive grain damage (Ref. 15). Thus, to preserve the internal structure of the samples, the thin-section techniques of petrography were used, although in addition some polished surfaces were also examined on a metallographic microscope (Ref. 16). Thin sections are made by grinding a substance that is opaque-to-translucent when thick to a thickness through which light is readily transmitted, permitting the internal crystalline and grain structure to be studied by transmitted polarized light (Ref. 17). With petrographic materials, this light transmission is achieved at a specimen thickness of 0.04 millimeter for most ceramics and rocks. This same thickness of material (less than the thickness of an average single explosive grain) was chosen for the explosive thin sections.<sup>1</sup>

<sup>1</sup> Naval Weapons Center. Projectile Impact Effects on the Physical Properties of TNT and Composition B, by Thomas A. Reitter, Carl F. Austin, and J. Kenneth Pringle. China Lake, Calif., NWC (in process).

The explosive thin sections were prepared for microscopic examination by cutting the test rod to yield the specific longitudinal or transverse sample desired. Transverse specimens were initially cut to yield a test piece having the diameter of the rod (2.13 centimeters) and a thickness of 0.8 centimeter. Longitudinal specimens were initially cut so as to be 2.13 centimeters wide, 1.9 centimeters long, and 0.8 centimeter thick. Each sample of explosive was then ground and polished by hand to yield a smooth surface which was sufficiently removed from the original saw cut to avoid grain damage caused by the cutting operations. The grinding routine called for 70-micron silicon carbide and water on a glass plate, followed by 15-micron silicon carbide on a glass plate, with a final polish using a paste of commercial polishing grade of magnesium oxide and water on a metallurgical cloth backed by a glass plate. The ground and polished specimen was cemented to a glass microscope slide which had been roughened on the specimen side by lightly grinding with 15-micron silicon carbide, followed by a rinse in dichromate glass-cleaning solution. Cementing of both the TNT and the Composition B-3 to the glass was successfully accomplished with a saturated solution of Lakeside 70C stick shellac dissolved in ethyl alcohol. At the time of cementing, an extra ring of shellac was placed around the outside edge of the specimen to serve as a seal to prevent the section of explosive from lifting from the glass and leaving air gaps into which the final grinding and polishing materials could enter. The grinding and polishing procedures were repeated on the exposed side of the explosive specimen until the final thickness of 0.04 millimeter was achieved. A commercial polishing grade of tin oxide was used prior to finishing with magnesium oxide in order to give faster grinding prior to the slower final polishing step. No cover glass was mounted on the slides. A cover glass was placed over the slide with distilled water during microscopic examinations to enhance light transmission, but was not left in place when the slides were restored.

#### IMPACT APPARATUS AND PROCEDURES

The experimental method for producing impact between a steel ball and the explosive test rods was similar to that described in Ref. 13 for inert materials, with the addition of personnel protection in the unlikely event that the test rods were accidentally to burn or detonate. A smooth-bore air gun with a maximum driving pressure of 13.6 atmospheres and a barrel diameter of 1.27 centimeters was mounted in a steel-lined port connecting a personnel barricade to an explosive test chamber in which the test rods of explosive were positioned (Fig. 3). The rods were placed on two semi-circular supports mounted upon a platform that was adjustable in height, tilt, and range. Both ends of the connecting port were protected by steel blast shields. The muzzle end of the gun barrel contained two sets of horizontal slits that permitted the passage of light from two bulbs onto two photocells and prevented further acceleration of the projectile, which was a hard steel sphere 1.27 centimeters in diameter. The interruption of these light beams by the passage of the projectile activated a time-

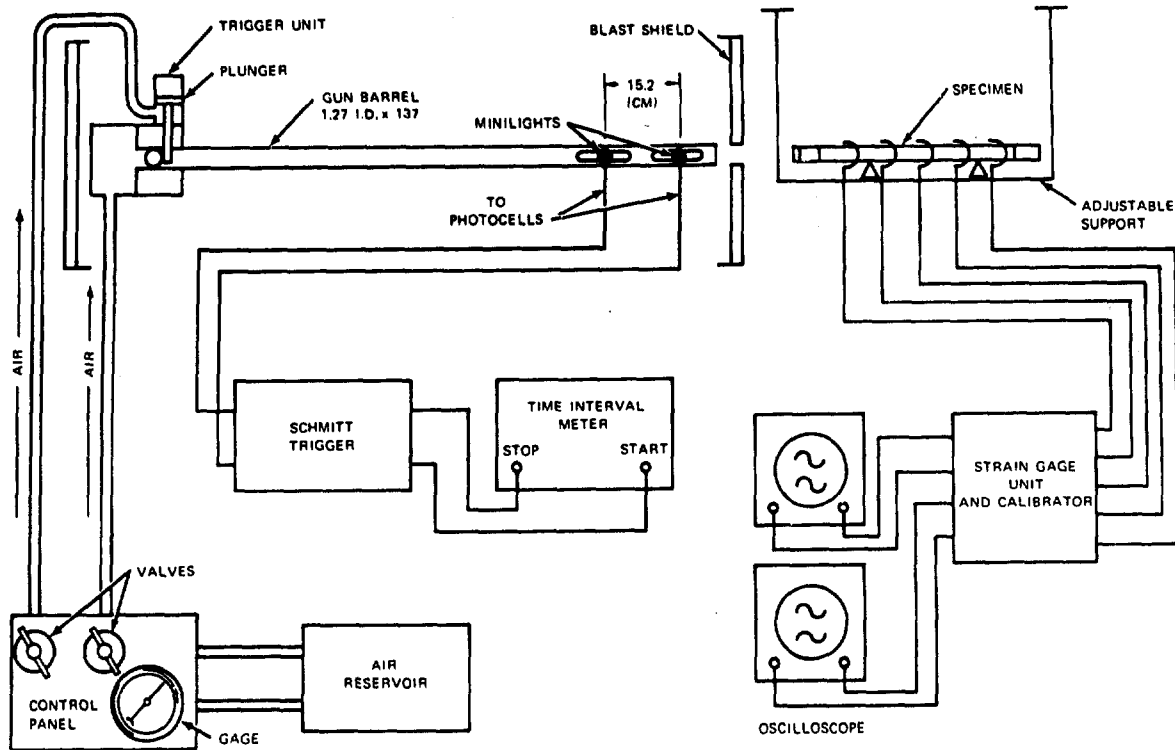


FIG. 3. Experimental Apparatus Used to Test the Response of Explosive Rods to Impact by Spherical Projectiles.

interval meter, which in turn permitted the calculation of the projectile velocity and initiated the delayed trigger pulse to the oscilloscopes that recorded the strain gage signals. The delay setting depended upon the initial velocity of the projectile.

Each target rod was brought separately to the explosive test chamber where the leads from the previously mounted strain gages were attached to the permanent potentiometric circuit leading to the oscilloscopes used to record the stress pulse passage. All diametrically opposite gages at a given station were connected in series to eliminate the antisymmetric component of the pulses. Prior to each shot, each strain gage channel was individually calibrated by noting the deflection of the oscilloscope traces upon the inclusion of known shunt resistances in the circuit.

Firing of the projectile was accomplished by first pressurizing a reservoir whose exit port was plugged by the steel ball and then pneumatically releasing a retaining pin which had kept the ball from moving down the gun barrel. Projectile velocity (26 to 150 m/sec) was controlled by the selection of the reservoir pressure.

## STATIC TEST PROCEDURES

Quasistatic tensile and compressive tests were performed both on an Instron (90-kilogram capacity) and a Tinius Olsen machine at a room temperature of 25.5°C. The explosive test assemblies (that is, explosive test rod and cemented-on screw ends) were attached to the pulling rods of the testing machines in such a way that a universal joint on each end of the pulling rods prevented bending in the assemblies being tested.

Tensile specimens were pulled to failure using a load cell and a recorder with a chart speed representing a multiple of the constant cross-head speed of 0.5 cm/min to record the test data automatically. The deflection of the test assembly was determined and subtracted from the motion of the crosshead in order to yield a value for the specimen deformation. The test assembly deflection was determined by a calibrated brass standard.

Static compressive tests consisted of squeezing the explosive specimens between a stationary and a moving platen until catastrophic failure occurred. The test assembly deflection for the compressive tests was negligible, as no complex pulling or squeezing assemblies were required. To verify this, a calibrated steel cylinder 5 centimeters in diameter was used to check the compression test assembly. The results of typical tensile and compressive tests are shown in Fig. 4, 5, and 6. The presence of glued joints was found to exert no influence on the results of any static or dynamic test.



FIG. 4. Samples of (A) TNT and (B) Composition B-3 Pulled to Failure in Tension.



FIG. 5. Sample of TNT Before and After Being Stressed to Failure in Compression. The moving platen was located at the top of the sample.



FIG. 6. Sample of Composition B-3 Stressed to Failure in Compression. The moving platen was located at the top of the sample.

## RESULTS

Static tensile, compressive, and dynamic tests were performed on samples of TNT and Composition B-3. The results of the static tests are shown in Tables 2 and 3. Typical static stress/strain curves for both virgin and shocked TNT and Composition B-3 were so similar they could not be readily distinguished; those shown in Fig. 7 and 8 are from shocked specimens.

Data from the dynamic tests are compiled in Tables 4 and 5. These tables list the test conditions, the strain amplitude of the initial pulse, the wave propagation velocity measured with respect to the pulse peaks, the amplitude of the tensile pulse ( $\sigma_T$ ) reflected from the distal end as modified by fractures and grain damage, the terminal permanent set ( $\epsilon_p$ ) evident at certain positions, and the average value of the dynamic Young's modulus ( $E_D$ ) calculated from the average density and average wave propagation velocity of the test materials.

Selected results of the Hopkinson bar experiments are presented in Fig. 9 and 10 for TNT and in Fig. 11 through 14 for Composition B-3, with the test configurations included. In these figures, fracture locations are shown by broken transverse lines in the sketches of specimen geometry. The time origin has been uniformly selected as the initial pulse arrival at the first strain gage station; the reference numbers for the various curves indicate the specific strain gage location depicted on the accompanying sketch.

Figures 9 and 11 show the effect of variations in the projectile velocity upon the propagation of the stress pulses through virgin test rods of TNT and Composition B-3, respectively, when both are struck under similar conditions. Test run K-1 is included in Fig. 11 in order to show the strain gage array for the Poisson ratio measurement at a position corresponding to gage 3 on the other test rods, requiring additional transverse gages to be mounted on rod K.

The effect of repeated impacts is shown in Fig. 10 for TNT and in Fig. 12 and 13 for Composition B-3. The two impacts on the TNT rod were made on the same end of the rod, but at different velocities. For the Composition B rod, two impacts were made on one end (Fig. 12) and two on the other (Fig. 13), all at essentially the same velocity.

The effect of the aluminum cap on the pulse amplitudes and shapes is shown in Fig. 9 and 14 for the two types of explosives tested. In conformity with the test results obtained for other substances, the presence of the protective metallic cap also served to increase the amplitude of the pulse at the first gage station in the case of the explosives, although not nearly to the same extent as with the inert silicates and ceramics (Ref. 9 and 10). On the other hand, the unprotected rods of explosive show a "permanent" strain of about 1,000 microstrain as

TABLE 2. Static Properties of Virgin Explosive Rods.

Sample <sup>a</sup>	Compressive stress at failure, bars	Initial compressive modulus, kbars	Tensile stress at failure, bars	Initial tensile modulus, kbars
Comp. B-3				
CB-1	160	60	...	...
CB-2	160	60	...	...
CB-3	150	60	...	...
CB-5	170	70	...	...
CB-6	180	80	...	...
CB-7	180	80	...	...
Average	170	70	...	...
TB-1	...	...	26	50
TB-2	...	...	26	30
TB-4	...	...	25	50
TB-5	...	...	24	50
Average	...	...	25	40
TNT				
CT-1	41	30	...	...
CT-2	60	40	...	...
CT-3	61	60	...	...
CT-4	63	60	...	...
CT-5	60	50	...	...
CT-6	54	40	...	...
CT-7	48	40	...	...
Average	55	50	...	...
TT-1 <sup>b</sup>	...	...	8.5	10
TT-2	...	...	7.5	20
TT-4	...	...	5.6	20
TT-5	...	...	4.9	8

<sup>a</sup> Samples were taken in succession along each rod. Where a sample number is missing, the sample was rejected due to machine malfunction or pretest damage.

<sup>b</sup> No averages are given for rod TT due to wide variation. The smaller crystals were at the end from which sample TT-1 was taken; the grain size became progressively larger as sample TT-5 was approached. This is evidenced by the steady decrease in tensile strength.

TABLE 3. Static Properties of Shocked Explosive Rods.

Sample <sup>a</sup>	Impact history of parent rod, velocity cm/sec	Distance of sample from impact end, <sup>b</sup> cm	Stress at failure, bar	Initial modulus, kbar
TNT				
S-C-1	14,900 & 14,500	15-20	73	30
S-C-2	14,900 & 14,500	33-38	56	30
U-C-1	14,100	8-10	70	30
U-C-2	14,100	38-42	50	30
T-C-1	14,100	15-20	72	40
T-C-2	14,100	28-33	68	40
R-C-1	11,400	13-15	68	40
YY-C-1	about 3,900 <sup>c</sup>	13-18	68	40
YY-C-2	about 3,900	33-38	53	30
YY-C-3	about 3,900	41-46 <sup>c</sup>	44	20
P-C-1	2,420 & 2,370	13-18	70	40
P-C-2	2,420 & 2,370	28-33	61	30
M-C-1	2,420	20-25	67	30
M-C-2	2,420	31-35	47	20
Comp. B-3				
I-C-1	15,600	15-20	150	50
I-C-2	15,600	30-33	160	50
G-C-1	15,500	13-15	160	50
G-C-2	15,500	28-30	150	50
D-C-1	4,200	10-15	160	60
D-C-2	4,200	28-33	180	60
D-C-3	4,200	36-40	190	70
E-C-1	Hit twice on one end at 2,450 and	0-5	170	60
E-C-2	2,470. Hit twice	8-13	150	50
E-C-3	on other end at	25-30	170	70
E-C-4	2,450 and 2,420.	33-38	170	60
F-C-1	2,380	2-7	180	80
F-C-2	2,380	30-35	160	80
F-C-3	2,380	38-43	170	80
I-T-1	15,600	10-13	21	30
I-T-2	15,600	23-25	18	30
D-T-1	4,200	0-8	17	40
D-T-2	4,200	15-20	18	30
E-T-1	Hit twice on one end at 2,450 and 2,470. Hit twice on other end at 2,450 and 2,420.	20-25	28	40
F-T-1	2,380	10-18	23	40
F-T-2	2,380	20-28	27	40
TNT				
S-T-1	14,900 & 14,500	5-13	6.8	10
S-T-2	14,900 & 14,500	25-33	6.7	20
U-T-1	14,100	20-23	2.3	10
U-T-2	14,100	30-35	3.9	10
R-T-1	11,400	20-25	5.2	30
YY-T-1	about 3,900	2-10	5.9	20
YY-T-2	about 3,900	18-25	5.1	10

<sup>a</sup> The first letter or pair of letters is the designation of the rod from which the samples were cut. The second letter, C or T, indicates compressive or tensile test. The number is the sample number.

<sup>b</sup> The "impact end" of a rod is the end first hit, regardless of whether the rod was later reversed.

<sup>c</sup> Rod YY was not instrumented and was 47 centimeters long.

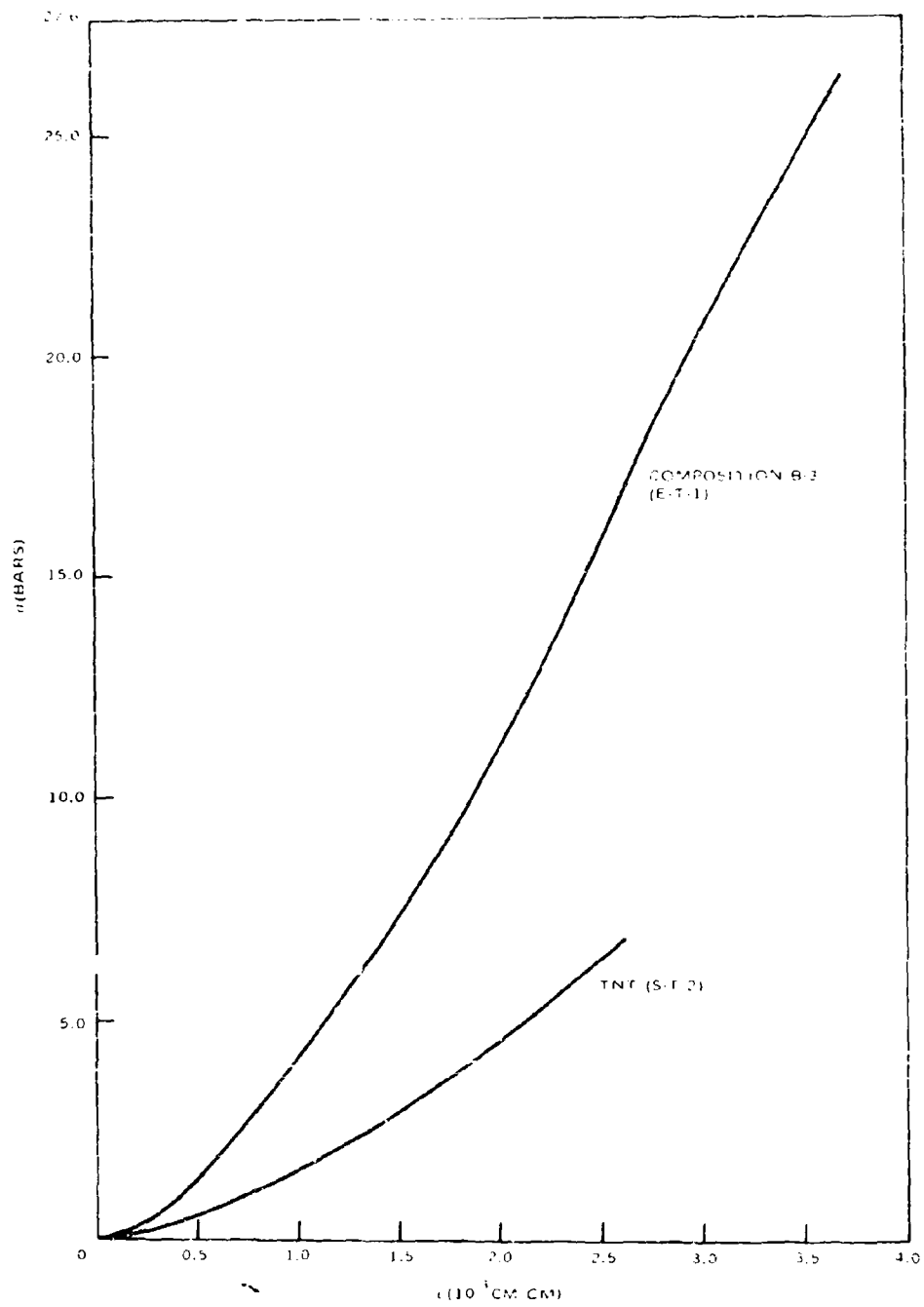


FIG. 7. Static Stress Strain Curves for Shocked TNT and Composition B-3 in tension.

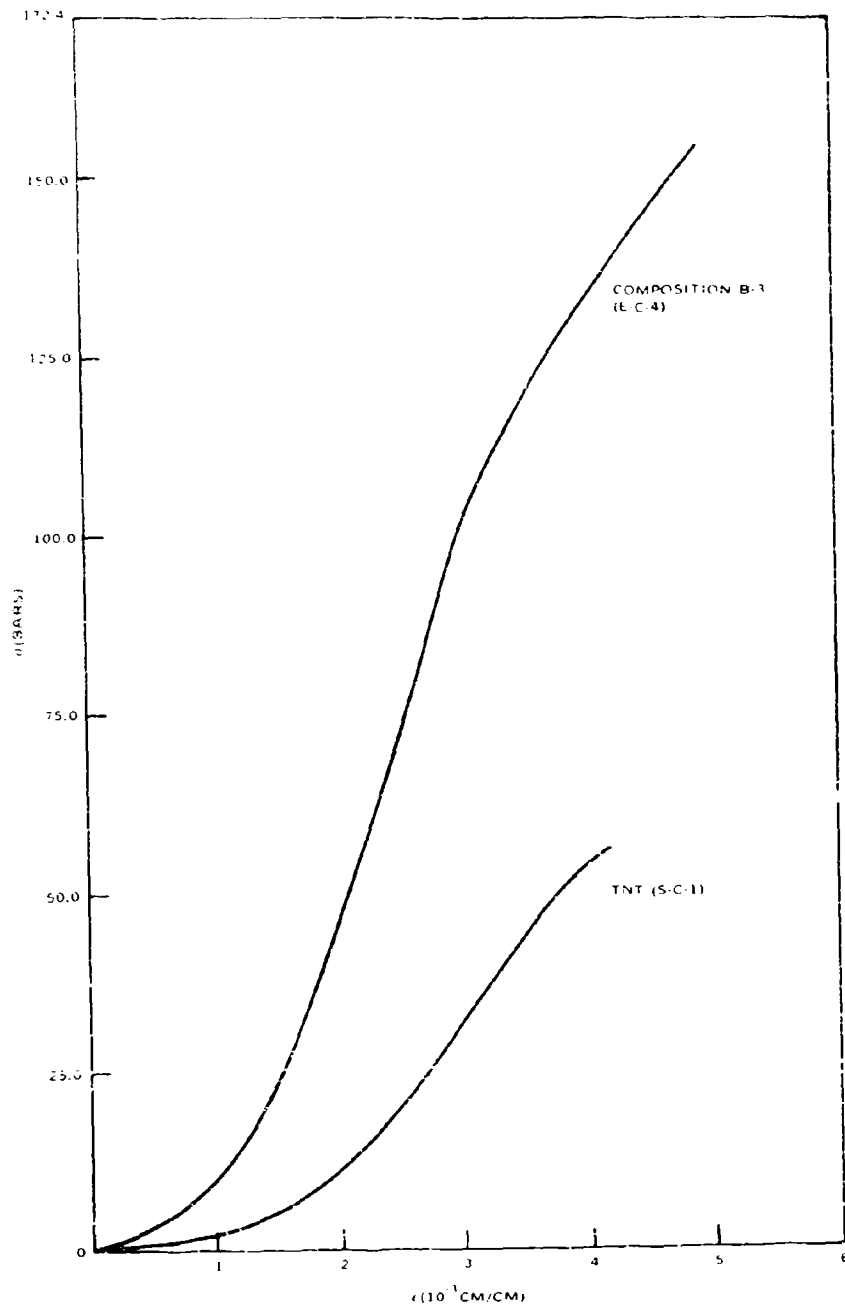


FIG. 8. Static Stress Strain Curves for Shocked Composition B-3 and TNT in Compression.

TABLE 4. Dynamic Properties of Composition B-3.

Test run	Initial projectile velocity, cm/sec	Al frontal piece	Strain amplitude of initial pulse at gage stations indicated, cm/cm $\times 10^{-3}$					ep: Permanent set, cm/cm $\times 10^{-6}$		$\sigma_T$ : Tensile wave amplitude, at gage stations indicated, bars					Wave propagation velocity between gage stations indicated, <sup>a</sup> cm/sec $\times 10^3$					Dynamic Poisson ratio				
			1	2	3 <sup>b</sup>	4	5	Gage interval	Strain	1	2	3	4	5	1-2	1-3	1-4	1-5	Average					
C-1	4,186	no	1.24	1.24	...	...	...	...	...	...	...	...	...	...	...	...	...	...	...	...	...	...	...	
D-1	4,196	yes	...	...	2.93	2.55	2.51	...	...	...	...	...	...	...	...	...	...	...	...	...	...	...	...	...
E-1	2,451	yes	3.36	2.84	2.48	2.02	...	200	1-3	200	55.4	...	...	222	247	249	...	...	...	...	...	...	240	
E-2	2,466	yes	1.27	1.14	1.16	0.98	0.74	570,580, 740	1-3	570,580, 740	20.0	3.1	24.8	20.0	3.1	222	241	254	258	...	...	...	...	243
E-3	2,451	yes	2.49	2.35	2.18	1.84	1.61	200	(1)	200	48.1	49.6	24.4	24.4	234	254	261	265	253	...	...	...	...	253
E-4	2,416	yes	1.50	1.30	...	0.55	0.30	...	...	...	...	...	...	...	235	...	213	212	220	...	...	...	...	220
F-1	2,380	yes	3.12	2.58	...	...	...	200,160	1-2	200,160	33.1	...	...	...	222	...	...	...	222	...	...	...	...	222
G-1	15,490	yes	4.29	3.60	3.20	...	...	...	...	...	...	...	...	...	247	240	...	...	244	...	...	...	...	244
H-1	15,420	no	2.62	2.14	1.96	1.80	1.70	1,100	1-5	1,100	33.4	...	4.8	4.8	212	214	222	225	218	...	...	...	...	218
I-1	15,620	yes	3.27	2.91	2.32	2.13	1.98	160	1-4	160	26.1	32.5	31.7	31.7	206	204	212	225	212	...	...	...	...	212
J-1	8,204	yes	2.64	2.09	1.79	1.66	1.44	160	1-2	160	11.4	6.5	21.2	21.2	212	212	214	218	214	...	...	...	...	214
K-1	2,400	yes	...	...	2.47	...	...	200	(1)	200	...	...	...	...	...	...	...	...	...	...	...	...	...	0.403
K-2	~14,000	yes	...	...	...	...	...	...	...	...	...	...	...	...	...	...	...	...	...	...	...	...	...	...
K-3	14,200	yes	...	...	...	...	...	...	...	...	...	...	...	...	...	...	...	...	...	...	...	...	...	...

<sup>a</sup>The average wave propagation velocity,  $\bar{C}_D$ , was  $225 \times 10^3$  cm/sec. The average sample density,  $\bar{\rho}$ , was  $1.718$  gm/cm<sup>3</sup>. From these values, the dynamic Young's modulus is calculated as  $E_D \equiv \bar{\rho} \bar{C}_D^2 = 86.8$  kilobars.

<sup>b</sup>Dual values for station 3, run K-1 denote longitudinal and transverse gage amplitudes, respectively.

TABLE 5. Dynamic Properties of TNT.

Test run	Initial projectile velocity, cm/sec	Al frontal piece	Strain amplitude of initial pulse at gage stations indicated, cm/cm $\times 10^{-3}$					ep: Permanent set, cm/cm $\times 10^{-6}$	$\sigma_T$ : Tensile wave amplitude, bars at gage stations indicated					Wave propagation velocity between gage stations indicated, cm/sec $\times 10^3$					Dynamic poisson ratio	
			1	2	3 <sup>b</sup>	4	5		Gage interval	Strain	1	2	3	4	5	1-2	1-3	1-4		1-5
M-1	2,421	yes	1.82	1.77	1.62	1.40	1.06	...	...	8.1	18.2	21.1	17.4	16.8	159	178	166	183	171	...
M-2	13,920	yes	1.95	1.92	1.65	1.41	...	(1)	400	...	16.8	28.0	28.7	...	212	204	207	...	208	...
P-1	2,426	yes	1.87	2.09	1.74	1.51	1.24	1-3	100	...	...	...	...	...	174	181	173	178	177	0.478
P-2	2,370	yes	2.05	1.96	1.67	...	1.36	...	...	...	...	...	...	185	207	...	196	196	0.423	...
R-1	11,400	yes	...	...	...	...	...	...	...	...	...	...	...	...	...	...	...	...	...	...
S-1	14,880	yes	...	...	...	...	...	...	...	...	...	...	...	...	...	...	...	...	...	...
S-2	14,530	yes	1.48	1.43	1.10	1.02	0.92	(1)	200	...	...	4.3	3.7	5.6	189	191	197	190	192	...
T-1	14,120	no	1.68	1.48	1.40	...	1.12	1-3	1,000	...	9.9	1.9	...	...	189	202	...	203	198	...
U-1	14,070	yes	2.03	1.64	1.54	...	1.07	1-2	200	...	...	6.2	...	27.2	198	184	...	185	189	...
Q-1	14,170	yes	...	1.42	1.48	1.27	1.02	...	...	...	21.1	18.7	31.1	...	...	198	191	201	196	...
V-1	8,738	yes	3.11	2.27	2.11	1.69	1.36	...	...	...	...	...	...	...	...	...	...	...	...	...

<sup>a</sup>The average wave propagation velocity,  $\bar{C}_D$ , was  $196 \times 10^3$  cm/sec. The average sample density,  $\bar{\rho}$ , was 1.629 gm/cm<sup>3</sup>. From these values, the dynamic Young's modulus is calculated as  $E_D \equiv \bar{\rho} \bar{C}_D^2 = 63.0$  kilobars.

<sup>b</sup>Dual values for station 2, runs P-1 and P-2 denote longitudinal and transverse gage amplitudes respectively.

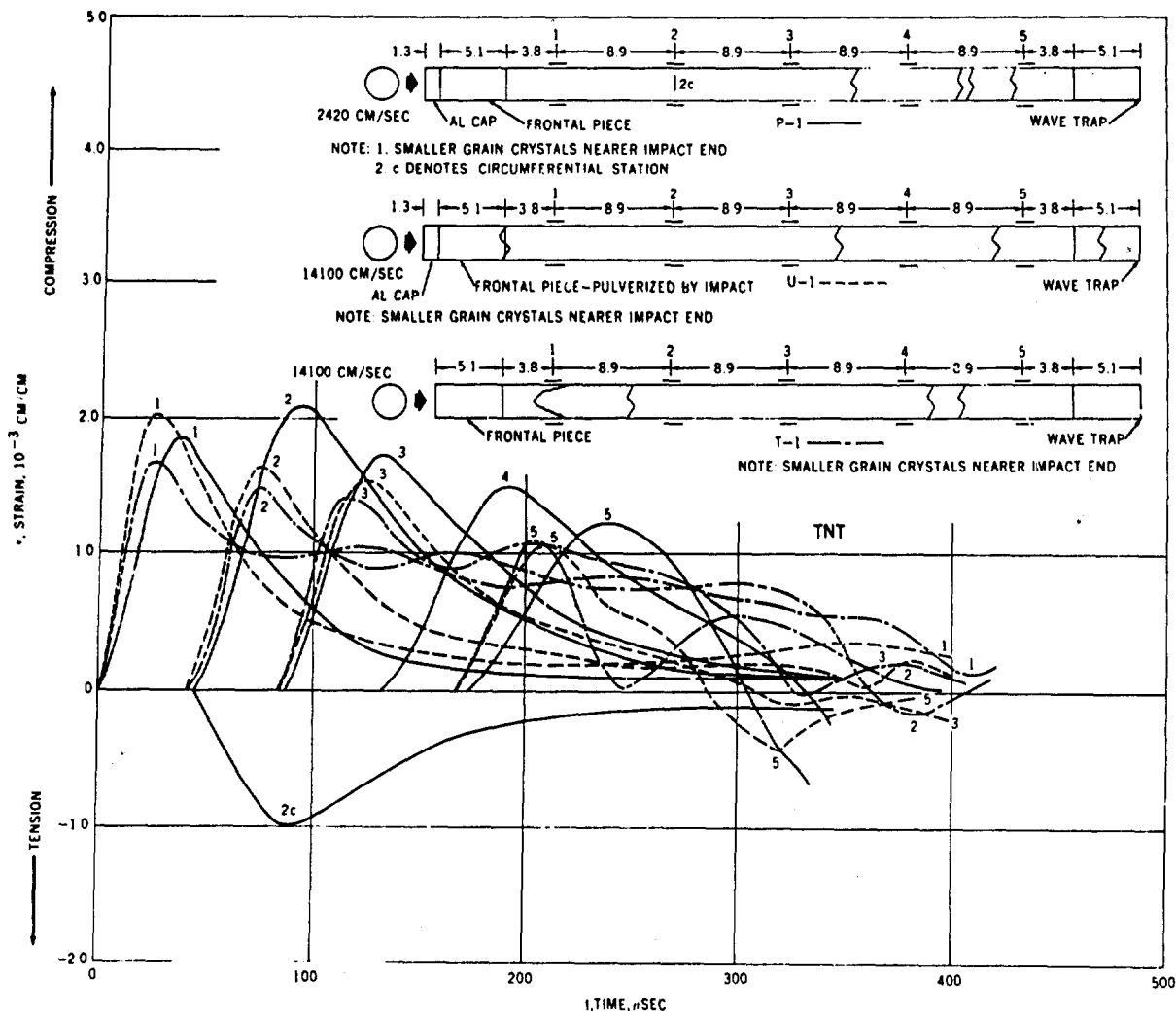


FIG. 9. Hopkinson Bar Test Results for the Impact at Two Velocities of a 1.27-Centimeter-Diameter Hard Steel Sphere Against 2.13-Centimeter-Diameter Rods of TNT. Rod dimensions are in centimeters.

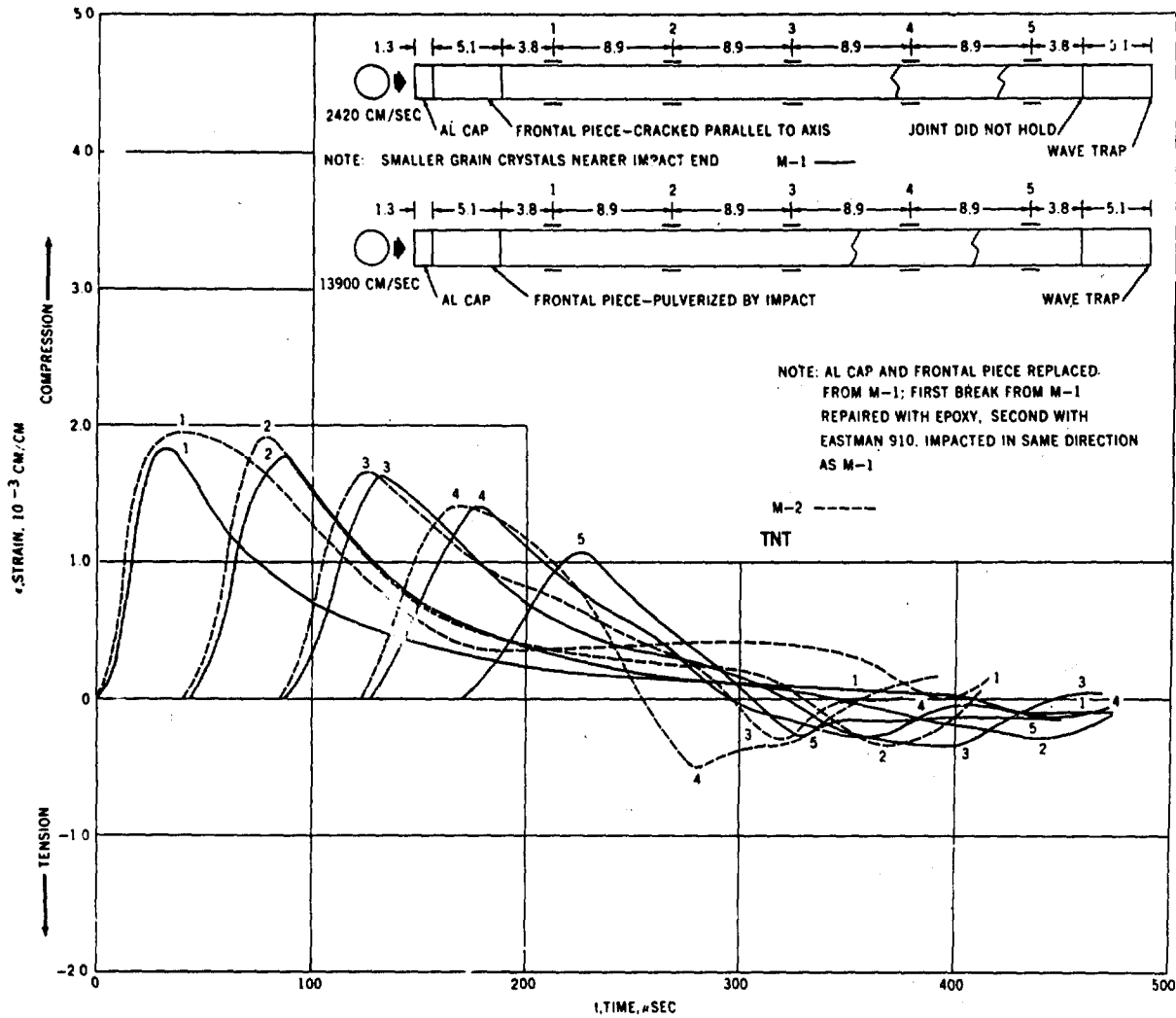


FIG. 10. Hopkinson Bar Test Results for the Repeated Impact of a 1.27-Centimeter-Diameter Hard Steel Sphere Against a Single 2.13-Centimeter-Diameter Rod of TNT. Rod dimensions are in centimeters.

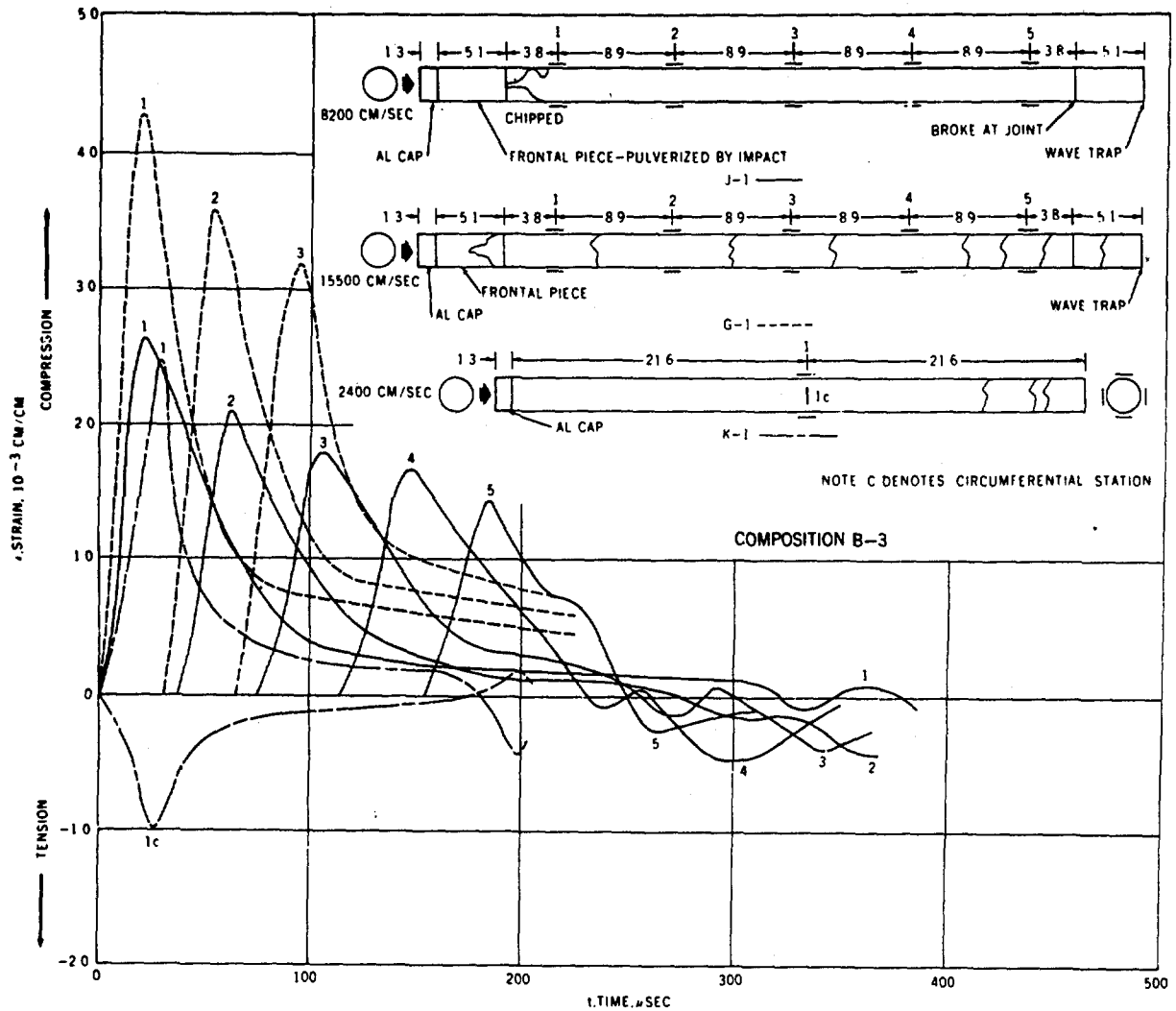


FIG. 11. Hopkinson Bar Test Results for the Impact at Three Velocities of a 1.27-Centimeter-Diameter Hard Steel Sphere Against 2.13-Centimeter-Diameter Virgin Rods of Composition B-3. Rod dimensions are in centimeters.

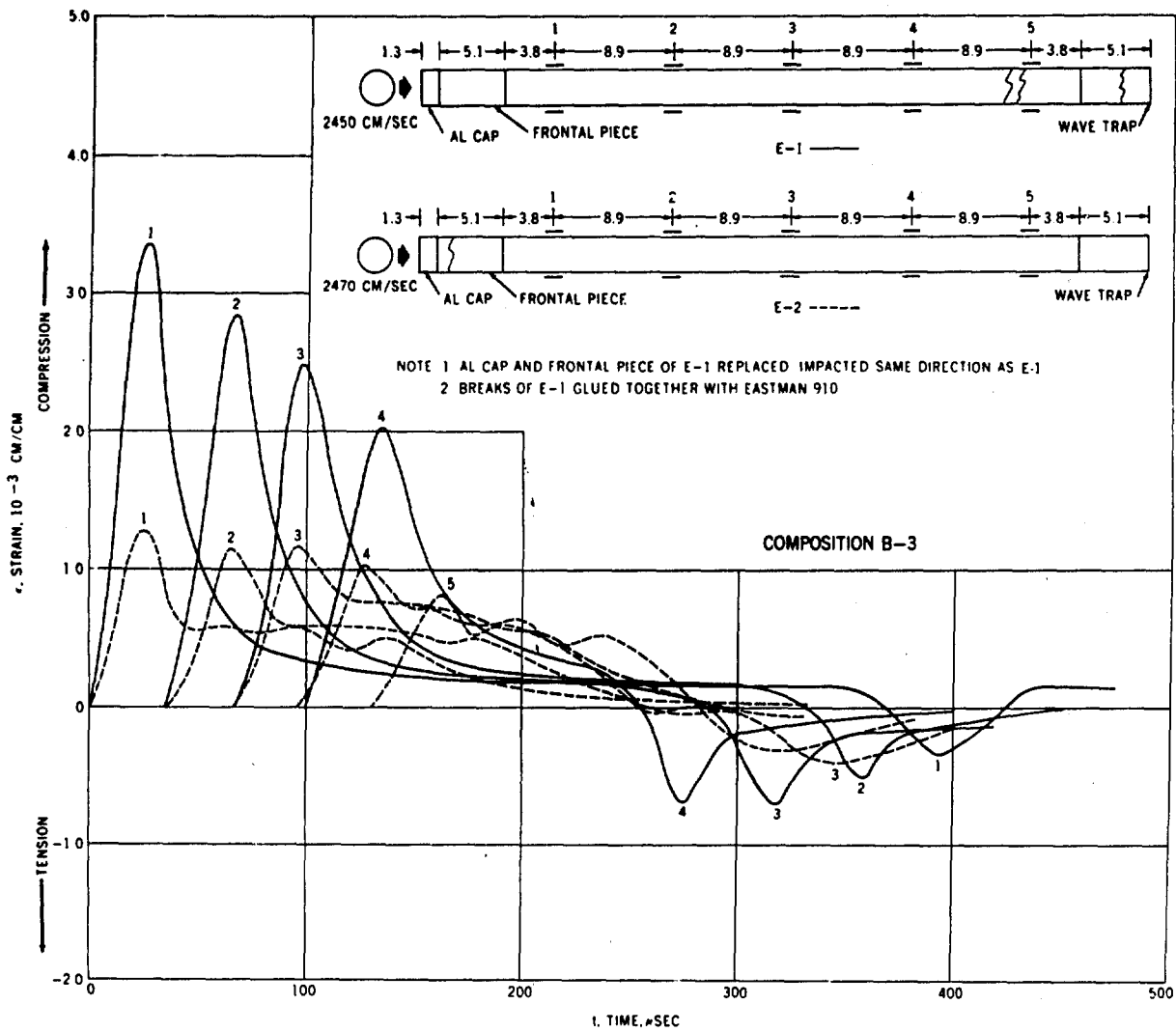


FIG. 12. Hopkinson Bar Test Results for the Repeated Impact of a 1.27-Centimeter-Diameter Hard Steel Sphere Against a Single 2.13-Centimeter-Diameter Rod of Composition B-3. Rod dimensions are in centimeters.

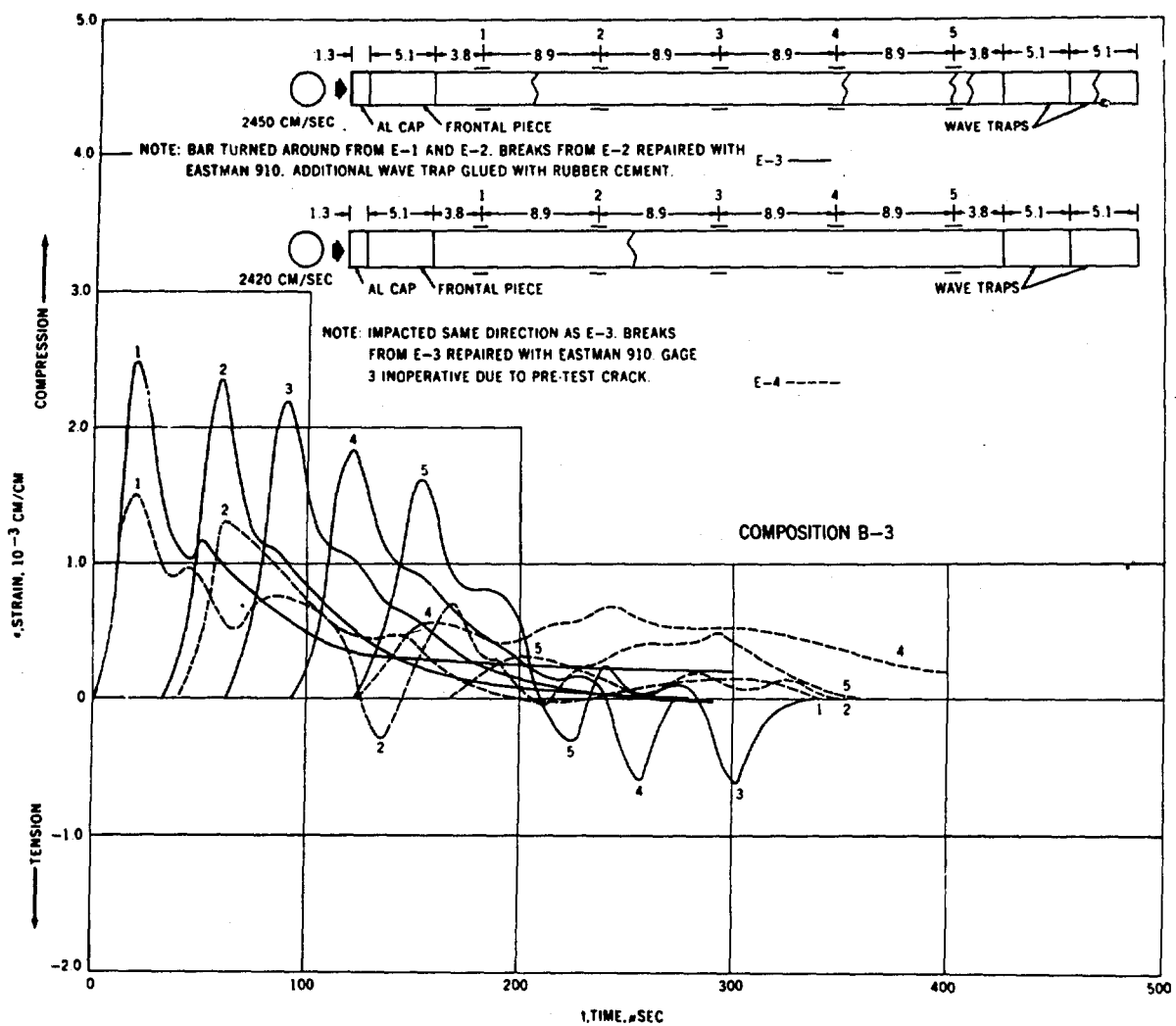


FIG. 13. Hopkinson Bar Test Results for Repeated Impact of a 1.27-Centimeter-Diameter Hard Steel Sphere Against a Single 2.13-Centimeter-Diameter Rod of Composition B-3. Rod dimensions are in centimeters.

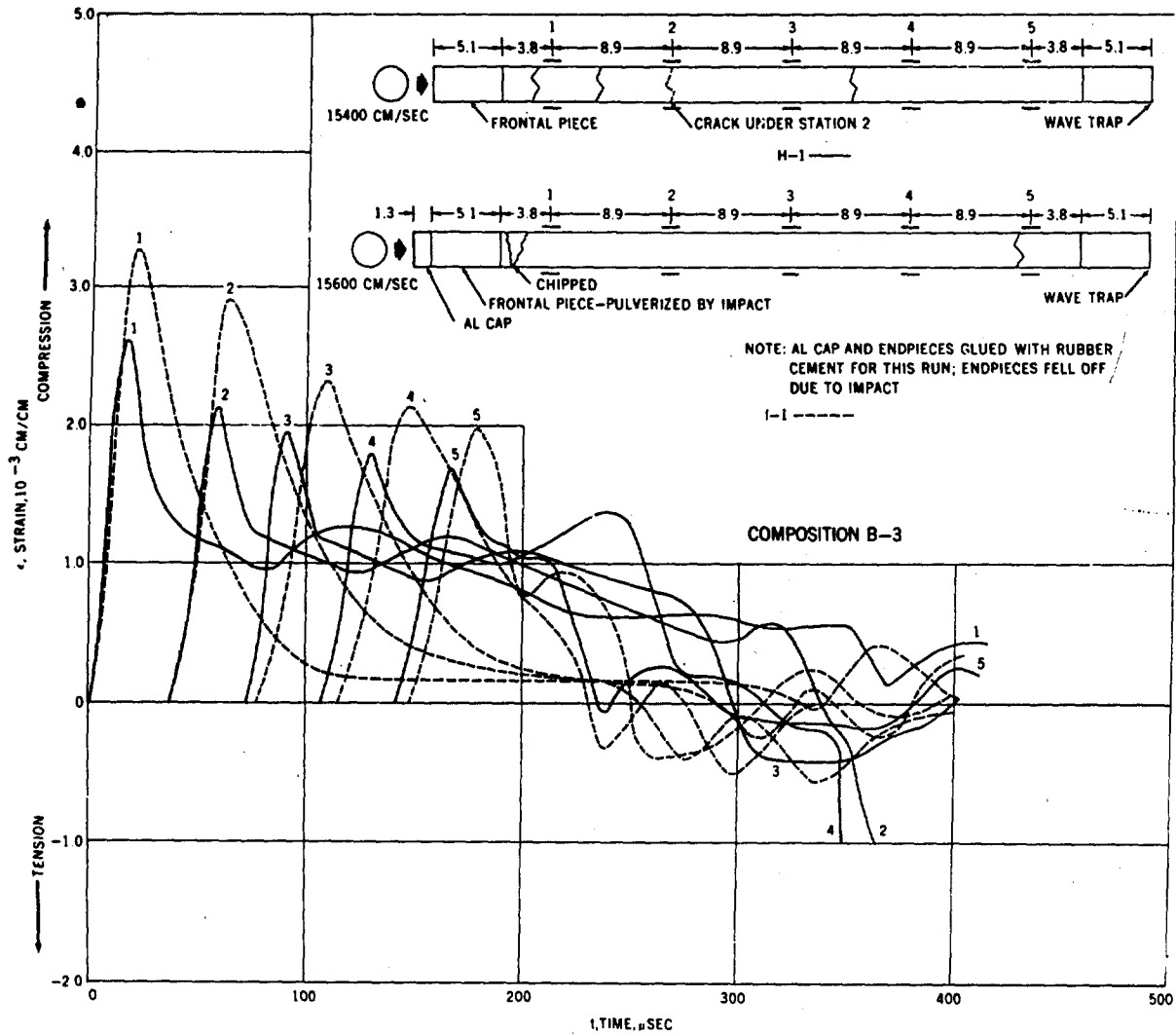


FIG. 14. Hopkinson Bar Test Results for the Impact at Two Velocities of a 1.27-Centimeter-Diameter Hard Steel Sphere Against 2.13-Centimeter-Diameter Rods of Composition B-3, Showing the Effect of Having an Aluminum Protector Cap. Rod dimensions are in centimeters.

evidenced in the records by a base-line shift immediately following the initial pulse, over the entire test rod, until the effect is obscured by reflection phenomena. With rods protected by aluminum caps, a similar permanent strain is seen to be confined to the vicinity of the impact point, with a magnitude not exceeding 200 microstrain, with the exception of the second impacts on rods E and M.

The study of the microscopic slides (thin sections) of the virgin and shocked specimens of TNT and Composition B-3 showed in great detail the crystalline fabric of all test specimens. Figures 15 and 16 present a transverse section of a virgin TNT test rod and the cross section of a shocked Composition B-3 test rod respectively. The cross section of virgin TNT test rods is composed of interpenetrating radial clusters of crystals, with the origin of the various radial arrays located on the outer surface of the rod. The outer 0.3 millimeter of rod thickness consists of a finer-grained layer which has filled in the area between the points of origin (nucleation) of the main groups of crystals. Penetration twins are common, and individual TNT crystals show abundant polysynthetic twinning. Some of the test rods show a more complex internal structure; that is, growth of individual larger TNT crystals was terminated by the formation of a rim of nearly parallel fine-grained acicular crystals of TNT. Larger TNT crystals occasionally show inclusions, often as rows down the crystal center, and also show occasional single needle-like crystal inclusions or clusters of slender crystals as inclusions. Although some of the intercrystal voids are due to plucking of the slide while it was being ground, the test rods appear to have both angular voids (intercrystal) and rounded voids (bubbles). A longitudinal section of a TNT rod shows the presence of the finer-grained skin, but does not show the prominent radial structure seen in cross sections. In view of the circular crystallite appearance of the rod exteriors, the internal structure must have resulted from crystal interference in three dimensions where the growing acicular bundles met and competed for space. Thus the appearance of a continuous thin skin of small crystals is somewhat misleading, especially in longitudinal sections and is, in part, the result of the cutting of random sections through the portion of the crystal bundles parallel to the rod mold surface. The TNT rods show no central void or shrinkage structure. Individual TNT crystals show mild internal strains in the form of undulatory extinctions.

The thin cross sections of Composition B-3 rods show the test specimens to be composed of fine-grained euhedral RDX crystals as inclusions in a generally coarse-grained TNT matrix. The TNT still exhibits the radial crystal pattern of the simple TNT rod cross sections, but does not appear to be as fine-grained near the rod edges; that is, a definite TNT skin is not evident. In some areas, the RDX is definitely oriented preferentially in accordance with the crystallographic directions of the host TNT crystals. This was seen in the cross sections as linear arrays of RDX which would go to extinction simultaneously. A definite flow alignment of the RDX crystals can be seen for the outermost few tenths of a



FIG. 15. Photomicrograph of a Thin Transverse Section of Virgin TNT With Edge of Rod in Lower Left Corner.



FIG. 16. Cross Section of a Shocked Test Rod of Composition B-3. Note the large fractured RDX crystal (arrow).

millimeter of rod, with the long axis of the RDX crystal, distinctly parallel to the walls of the test rod. The Composition B-3 test rods sectioned do not show a centrally positioned TNT core, probably due to the influence of adjacent molds on the heat loss history of individual molds. A typical Composition B-3 rod showed a 0.3-millimeter-diameter, slightly elliptic core of RDX-free TNT as a radial crystal array nearly one-third of the way in from one edge. Individual RDX crystals show slightly wavy extinctions, indicating some strain, and the large TNT crystals appear to do the same.

Because of the inherent crystallization properties of the two explosives studied, the strain gages were cemented onto somewhat oriented textures in the Composition B-3. For the TNT rods, mixtures of fine-grained crystals and flat radial sprays of acicular TNT crystals represented the outer surface.

The thin sections of shocked explosives were evaluated for the effects of the passage of stress waves. The examination and interpretation of fractures seen in thin sections is complicated by the probable presence of three types of fractures: dynamic from the tests, static from shrinkage and internal stress during rod fabrication, and static from the thin-section cutting and grinding processes. With the present state of the art for making and interpreting thin sections of shocked explosives, only the most prominent visual effects can be reported.

Shocked TNT differed in thin section from virgin TNT by the presence of widespread pits and fractures in the former, indicating failure of crystals along cleavages or partings. This pitting was not evident at the distal end of a rod struck twice at 149 and 145 m/sec, respectively (test run S), but was very prominent in a section near the point of impact.

The failure of Composition B-3 was evidenced by widespread fracturing, combined with grain-bond failures and internal cracking of the RDX. One sample (test run K) was macroscopically cracked by impact prior to sectioning. Examination of these fractures showed a tendency for those passing through RDX grains to deflect and for fractures to the side of a main through-going fracture to be strongly controlled by local crystal orientation. Shattering of individual RDX crystals was seen along a minor fracture, but was not observed on the main through-going fracture (which could conceivably have been formed quasistatically by the delayed release of stored strain after impact). Some straight-line fractures in the Composition B-3 test specimens were obviously controlled in orientation by the crystal structure of the coarse-grained TNT matrix.

The use of an alcohol/shellac cement in the preparation of the microscopic slides might be criticized in view of the slight solubility of TNT in this liquid. On the other hand, other common adhesives entail the employment of even stronger solvents and elevated temperatures incompatible with the explosive, or else they have one or more crystalline

component themselves. Microscopic investigation showed no degradation of the slides due to the use of alcohol in mounting.

#### DISCUSSION

The microstructures of TNT and Composition B-3 show abundant physical damage near areas of impact, in the form of cracking, grain-bond separation, and extensive weakening of cleavages or partings. Macroscopic examination of the shocked rods clearly showed damage near impact areas in the form of scattered fractures, plus the discoloration due to internal grain breakup.

No obvious trends are apparent from the results of the static tensile tests, but as with other brittle materials studied by these methods, the variation in strength properties from specimen to specimen was of the order of the magnitude of the failure stress and hence, it obscured any significant trends. On the other hand, some general observations can be made about the compressive tests. For Composition B-3, the ultimate strength of both virgin and shocked specimens was about the same. The Young's modulus of the virgin specimens was also comparable to the modulus of samples shocked at velocities of less than 150 m/sec, even when repeatedly shocked, and was only slightly higher than that of specimens shocked at the upper test velocity of 150 m/sec. For TNT, the static strengths of the virgin and shocked specimens were comparable, but the Young's modulus of the shocked specimens was lower. In particular, the modulus of rods which had suffered multiple impacts was considerably reduced.

The results of the dynamic tests reveal a significant attenuation of the pulse with travel distance for both materials. A considerably greater attenuation occurred with TNT, possibly due to the coarse crystal size combined with through-going cleavages, whereas in Composition B-3 these cleavages were interrupted by the dispersed RDX crystals. Less correlation was observed between impact velocity and strain level than for any other nonmetallic substance studied by the authors. This lack of correlation may be partially due to the relatively high anelastic nature of the explosives, but is believed to be primarily the result of the poor degree of internal structural control that was exercised in the manufacturing and preparation of the explosive test bars.

There is some noticeable dispersion in the pulse shapes. For Composition B, an exponential pulse peak decay is a reasonably good fit with a coefficient of 0.0145/cm, whereas a similar decay value cannot be assigned to TNT because of its inconsistent behavior. In terms of transit distance the average decay for the two materials in 35 centimeters was about 40%, with noticeable dispersion in addition to the attenuation. Figure 17 presents a nondimensional plot of the attenuation of the two explosives compared with a variety of natural and artificial nonmetallic substances subjected to mechanical impacts of about the same strain magnitude. The

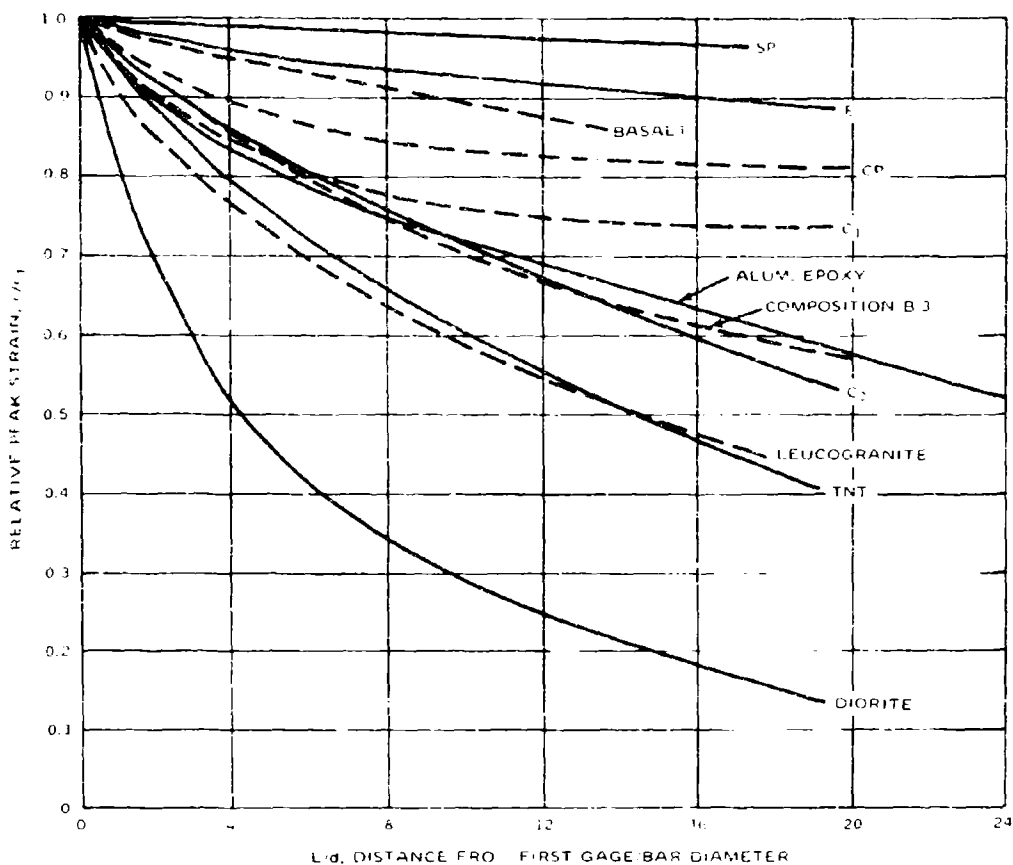


FIG. 17. Comparison of Wave Attenuation in Composition B ( $3.27 \times 10^{-3}$  cm/cm) and TNT ( $3.11 \times 10^{-3}$  cm/cm) With Various Inert Materials: SP (Spessartite at  $1.4 \times 10^{-3}$  cm/cm), E (epoxy at  $7.3 \times 10^{-3}$  cm/cm), C<sub>1</sub> (model concrete  $0.95 \times 10^{-3}$  cm/cm), CP (cement paste at  $1.75 \times 10^{-3}$  cm/cm), Basalt ( $1.3 \times 10^{-3}$  cm/cm), Aluminum Epoxy ( $3.2 \times 10^{-3}$  cm/cm), Leucogranite ( $1.5 \times 10^{-3}$  cm/cm), and Diorite ( $2.0 \times 10^{-3}$  cm/cm). The numerical value is given for peak strain at the first gage station (Ref. 9).

reduction in amplitude found with stress pulse passage in TNT (test run V-1) and Composition B-3 (test run I-1) is similar to that found in an equal mixture of aluminum powder and an epoxy (diepoxide plus filler and unfilled polysulfide hardener containing an accelerator in a ratio of 2.5:1 by volume). Unlike other nonmetallics, there is no definitive trend toward larger pulse attenuation at higher strain amplitudes in either TNT or Composition B-3 within the velocity range employed.

Both explosives differed very sharply in their mechanical properties from the various inert nonmetallics previously studied, including rocks, artificial concretes, cements, and epoxy mixtures. The density and rod wave velocity, and hence the acoustic impedance,  $\rho c_0$ , are considerably less than those for either nonvesicular igneous rocks or for model concrete. The Composition B-3 tested had an acoustic impedance of 386 gm-sec/cm<sup>3</sup>, and TNT had a value of 319 gm-sec/cm<sup>3</sup>, whereas model concrete had a value of 807 gm-sec/cm<sup>3</sup>. In contrast, the values of Poisson's ratio for both explosives were in excess of 0.4; this is well beyond the range of any of the rocks or cementitious mixtures previously analyzed and is comparable to that found for plastic compounds whose behavior on a macroscopic level is generally regarded as viscoelastic.

The peak amplitudes of the reflected waves are not necessarily a direct indication of the dynamic tensile strength of the materials tested. One reason is that specimen or gage breakage may occur due to reasons other than fracture by the particular pulse component undergoing evaluation. Another is that peak amplitudes are subject to the random variations of strength properties inherent in granular brittle materials undergoing tensile failure. However, a reasonable average for this parameter is 30 bars for Composition B-3 and 20 bars for TNT. These values are roughly comparable to the static values determined for the test rods.

#### CONCLUSIONS

From the static and dynamic tests of Hopkinson bars composed of rods of cast Composition B-3 and cast TNT, the following conclusions can be drawn:

1. Strain pulses attenuate and disperse with travel distance in rods of these materials, indicating that a macroscopic constitutive equation for these solids must take into account the viscoelastic behavior of the materials. The absence of correlation between the initial impact velocity and the resultant peak strain at the first observation station indicates that the material behavior is probably nonlinear.

2. The static strength properties of the materials did not seem to be significantly affected by prior impacts using spherical steel projectiles with a diameter of 1.27 centimeters at initial velocities up to 150 m/sec, although the Young's moduli were somewhat decreased under these circumstances.

3. Severe internal damage to the specimens was caused by the shocks. Microscopic examination revealed widespread crystalline damage and grain-bond failure near the point of impact. TNT crystals showed extensive failure along cleavages or partings; Composition 8-3 showed failure of the TNT as well as fracturing through and around RDX grains and, less commonly, within individual RDX grains.

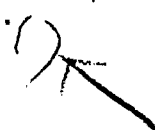
## REFERENCES

1. U.S. Naval Ordnance Test Station. Transactions of the Symposium on Warhead Research (Surface Targets)(U). China Lake, Calif., NOTS, September 1962. (NOTS TP 2958, publication CONFIDENTIAL.) Pp. 263-76.
2. Wood, Col. John S., Jr. "Future Infantry Arms," ORDNANCE, July-August 1969, pp. 74-77.
3. Eglin Air Force Base. Impact Sensitivity and Cratering Test of the Mk 84 Mod 1 2000-lb. General Purpose Bomb (U), by Philip P. Face. EAFB, Florida, November 1967. (APGC-TR-67-135, publication CONF.)
4. Naval Weapons Laboratory. Review of Development and Evaluation of Warhead EX 29 Mod 3 (Prototype Mk 19 Mod 0)(U), by J. J. Clancy. Dahlgren, Va., NWL, November 1959. (No. T-43/59, publication CONF.)
5. Aberdeen Proving Ground, Maryland. "Test of Shell HE 105 MM, M1 With Various Fillers Against Concrete," Third Report on Project No. TA 1-3501, 19 November 1954.
6. U.S. Naval Ordnance Test Station. Some Dynamic Characteristics of Rocks, by Werner Goldsmith and Carl F. Austin. China Lake, Calif., NOTS, May 1963. (NOTS TP 3205.) 35 pp. Also in Stress Waves in Anelastic Solids. Berlin, Springer Verlag, 1964. P. 277.
7. -----. Dynamic Behavior of Concrete, by Werner Goldsmith, Milos Polivka, and Ta-Lun Yang. China Lake, Calif., NOTS, October 1965. (NOTS TP 3890.) 42 pp. Also in EXP MECH, Vol. 6, No. 2 (1966), p. 65.
8. -----. Stress Wave Passage in Selected Rock Fabrics, by Carl F. Austin, Werner Goldsmith, and Stephen Finnegan. China Lake, Calif., NOTS, June 1965. (NOTS TP 3793.) 66 pp.
9. Goldsmith, W., V. H. Kenner and T. E. Ricketts. "Dynamic Loading of Several Concrete-Like Mixtures," Journal of the Structural Division, AMER SOC CIVIL ENG, PROC, No. 6041 (July 1968), p. 1803.
10. Ricketts, T. E., and W. Goldsmith. International Journal of Rock Mechanics. (In press.)

11. Naval Weapons Center. Transactions of the Fifth NWC Warhead Research and Development Symposium (U). China Lake, Calif., NWC, December 1967. (NWC TP 4446, Vol. 2, publication CONFIDENTIAL.) Pp. 25-1.
12. U.S. Naval Ordnance Test Station. Transactions of the Fourth Symposium on Warhead Research (U). China Lake, Calif., NOTS, June 1966. (NOTS TP 3984, publication CONFIDENTIAL.) Pp. 150-64.
13. Goldsmith, Werner, Carl F. Austin, Cheh-Cheng Wang, and Stephen A. Finnegan. "Stress Waves in Igneous Rocks," J GEOPHYS RES, Vol. 71, No. 8 (15 April 1966), pp. 2055-78.
14. Griffiths, N., R. McN. Laidler, and T. S. Spenser. "Some Aspects of the Shock Initiation of Explosives," COMBUST AND FLAME, Vol. 7, No. 4 (December 1963), pp. 347-52.
15. Williamson, W. O. "The Crystalline Arrangement in Fusion-Cast Cylinders of 2:4:6-Trinitrotoluene and its Relationship to Colour, Density and Behaviour on Detonation," J APPL CHEM (London), No. 8 (June 1958) pp. 367-75.
16. Connick, W., and B. W. Thorpe. "An Improved Technique for the Mechanical Polishing of RDX/TNT." Department of Supply, Australian Defence Scientific Service, Defence Standards Laboratories, Maribyrnong, Victoria, August 1968. (Technical Note 119.)
17. Rogers, Austin F., and Paul F. Kerr. Optical Mineralogy. New York, McGraw-Hill, 1942.

**UNCLASSIFIED**

Security Classification

DOCUMENT CONTROL DATA - R&D		
<i>(Security classification of title, body of abstract and indexing annotation must be entered when the overall report is classified)</i>		
1. ORIGINATING ACTIVITY (Corporate author) Naval Weapons Center China Lake, California 93555		2a. REPORT SECURITY CLASSIFICATION <b>UNCLASSIFIED</b>
		2b. GROUP
3. REPORT TITLE <b>STATIC AND DYNAMIC PROPERTIES OF TWO EXPLOSIVE MATERIALS</b>		
4. DESCRIPTIVE NOTES (Type of report and inclusive dates) <b>Research Report</b>		
5. AUTHOR(S) (Last name, first name, initial) <b>Goldsmith, Werner; Reitter, Thomas A.; Austin, Carl F.</b>		
6. REPORT DATE <b>January 1970</b>	7a. TOTAL NO. OF PAGES <b>34</b>	7b. NO. OF REFS <b>17</b>
8a. CONTRACT OR GRANT NO.	9a. ORIGINATOR'S REPORT NUMBER(S) <b>NWC TP 4805</b>	
b. PROJECT NO.	9b. OTHER REPORT NO(S) (Any other numbers that may be assigned this report)	
c. <b>NAVAIR A35-350/216/70 F17353501</b>		
d.		
10. AVAILABILITY/LIMITATION NOTICES <b>This document is subject to special export controls and each transmittal to foreign governments or foreign nationals may be made only with prior approval of the Naval Weapons Center.</b>		
11. SUPPLEMENTARY NOTES	12. SPONSORING MILITARY ACTIVITY <b>Naval Air Systems Command Department of the Navy Washington, D. C. 20360</b>	
13. ABSTRACT <p>↘ Test rods of Composition B-3 and TNT were cast 43.2 centimeters long and 2.13 centimeters in diameter. The rods were struck axially by spherical steel projectiles, and symmetric stress wave passage was observed by strain gage arrays. Strain pulses were found to attenuate and disperse with travel distance. Both damaged and undamaged rods were examined microscopically using thin-section techniques and were also tested for static compressive and tensile strength. The thin-section technique was able to show grain and crystal damage resulting from impacts. A macroscopic constitutive equation for these materials must take into account their anelastic behavior.</p> 		

DD FORM 1473

1 JAN 64

0101-807-6800

Security Classification

14. KEY WORDS	LINK A		LINK B		LINK C	
	ROLE	WT	ROLE	WT	ROLE	WT
Explosives Impact damage Stress waves Attenuation Thin sections Grain structure TNT Composition B						

**INSTRUCTIONS**

1. **ORIGINATING ACTIVITY:** Enter the name and address of the contractor, subcontractor, grantee, Department of Defense activity or other organization (*corporate author*) issuing the report.
- 2a. **REPORT SECURITY CLASSIFICATION:** Enter the overall security classification of the report. Indicate whether "Restricted Data" is included. Marking is to be in accordance with appropriate security regulations.
- 2b. **GROUP:** Automatic downgrading is specified in DoD Directive 5200.10 and Armed Forces Industrial Manual. Enter the group number. Also, when applicable, show that optional markings have been used for Group 3 and Group 4 as authorized.
3. **REPORT TITLE:** Enter the complete report title in all capital letters. Titles in all cases should be unclassified. If a meaningful title cannot be selected without classification, show title classification in all capitals in parentheses immediately following the title.
4. **DESCRIPTIVE NOTES:** If appropriate, enter the type of report, e.g., interim, progress, summary, annual, or final. Give the inclusive dates when a specific reporting period is covered.
5. **AUTHOR(S):** Enter the name(s) of author(s) as shown on or in the report. Enter last name, first name, middle initial. If military, show rank and branch of service. The name of the principal author is an absolute minimum requirement.
6. **REPORT DATE:** Enter the date of the report as day, month, year, or month, year. If more than one date appears on the report, use date of publication.
- 7a. **TOTAL NUMBER OF PAGES:** The total page count should follow normal pagination procedures, i.e., enter the number of pages containing information.
- 7b. **NUMBER OF REFERENCES:** Enter the total number of references cited in the report.
- 8a. **CONTRACT OR GRANT NUMBER:** If appropriate, enter the applicable number of the contract or grant under which the report was written.
- 8b, 8c, & 8d. **PROJECT NUMBER:** Enter the appropriate military department identification, such as project number, subproject number, system numbers, task number, etc.
- 9a. **ORIGINATOR'S REPORT NUMBER(S):** Enter the official report number by which the document will be identified and controlled by the originating activity. This number must be unique to this report.
- 9b. **OTHER REPORT NUMBER(S):** If the report has been assigned any other report numbers (*either by the originator or by the sponsor*), also enter this number(s).
10. **AVAILABILITY/LIMITATION NOTICES:** Enter any limitations on further dissemination of the report, other than those

imposed by security classification, using standard statements such as:

- (1) "Qualified requesters may obtain copies of this report from DDC."
- (2) "Foreign announcement and dissemination of this report by DDC is not authorized."
- (3) "U. S. Government agencies may obtain copies of this report directly from DDC. Other qualified DDC users shall request through \_\_\_\_\_."
- (4) "U. S. military agencies may obtain copies of this report directly from DDC. Other qualified users shall request through \_\_\_\_\_."
- (5) "All distribution of this report is controlled. Qualified DDC users shall request through \_\_\_\_\_."

If the report has been furnished to the Office of Technical Services, Department of Commerce, for sale to the public, indicate this fact and enter the price, if known.

11. **SUPPLEMENTARY NOTES:** Use for additional explanatory notes.

12. **SPONSORING MILITARY ACTIVITY:** Enter the name of the departmental project office or laboratory sponsoring (*paying for*) the research and development. Include address.

13. **ABSTRACT:** Enter an abstract giving a brief and factual summary of the document indicative of the report, even though it may also appear elsewhere in the body of the technical report. If additional space is required, a continuation sheet shall be attached.

It is highly desirable that the abstract of classified reports be unclassified. Each paragraph of the abstract shall end with an indication of the military security classification of the information in the paragraph, represented as (TS), (S), (C), or (U).

There is no limitation on the length of the abstract. However, the suggested length is from 150 to 225 words.

14. **KEY WORDS:** Key words are technically meaningful terms or short phrases that characterize a report and may be used as index entries for cataloging the report. Key words must be selected so that no security classification is required. Identifiers, such as equipment model designation, trade name, military project code name, geographic location, may be used as key words but will be followed by an indication of technical context. The assignment of links, roles, and weights is optional.